

# Comparative Reliability Analysis of Publicly Available Software Packages for Automatic Intracranial Volume Estimation

S. Sargolzaei, M. Goryawala, M. Cabrerizo, G. Chen, P. Jayakar, R. Duara, W. Barker, M. Adjouadi

**Abstract**— Intracranial volume is an important measure in brain research often used as a correction factor in inter subject studies. The current study investigates the resulting outcome in terms of the type of software used for automatically estimating ICV measure. Five groups of 70 subjects are considered, including adult controls (AC) (n=11), adult with dementia (AD) (n=11), pediatric controls (PC) (n=18) and two groups of pediatric epilepsy subjects (PE1.5 and PE3) (n=30) using 1.5 T and 3T scanners, respectively. Reference measurements were calculated for each subject by manually tracing intracranial cavity without sub-sampling. Four publicly available software packages (AFNI, Freesurfer, FSL, and SPM) were examined in their ability to automatically estimate ICV across the five groups. Linear regression analyses suggest that reference measurement discrepancy could be explained best by SPM [ $R^2 = 0.67$ ;  $p < 0.01$ ] for the AC group, Freesurfer [ $R^2 = 0.46$ ;  $p = 0.02$ ] for the AD group, AFNI [ $R^2 = 0.97$ ;  $p < 0.01$ ] for the PC group and FSL [ $R^2 = 0.6$ ;  $p = 0.1$ ] for the PE1.5 and [ $R^2 = 0.6$ ;  $p < 0.01$ ] for PE3 groups. The study demonstrates that the choice of the automated software for ICV estimation is dependent on the population under consideration and whether the software used is atlas-based or not.

## I. INTRODUCTION

Intracranial volume (ICV), sometimes referred to as total intracranial volume (TIV), refers to the estimated volume of cranial cavity as outlined by the supratentorial dura matter or cerebral contour when dura matter is not clearly detectable [1, 2]. ICV is often used in studies involved with analysis of the cerebral structure under different imaging modalities, such as Magnetic Resonance (MR) [3], MR and Diffusion Tensor Imaging (DTI) [4], MR and Single-Photon Emission Computed Tomography (SPECT) [5], Ultrasound [6] and Computerized Tomography (CT) [7, 8]. ICV consistency during aging [9] makes it a reliable tool for correction of head size variation across subjects in studies that rely on

S. Sargolzaei and M. Goryawala are with the center for Advanced Technology and Education (CATE), Florida International University, Miami, FL 33174 USA (phone: 303-348-4106; e-mail: ssarg004@fiu.edu).

M. Cabrerizo is the Mark Edwards Assistant Professor in Neuroscience and Learning with the center for Advanced Technology and Education (CATE), Department of Electrical and Computer Engineering, Florida International University, Miami, FL 33174 USA.

G. Chen is with the scientific and statistical computing core at NIMH/NIH/ HHS, Bethesda, MD 20892 USA.

P. Jayakar is with the Brain institute at Miami Children's Hospital, Miami, FL 33155, USA.

R. Duara and W. Barker are with the Wien Center for Alzheimer's Disease and Memory Disorders, Mount Sinai Medical center, Miami Beach, FL 33140.

M. Adjouadi is Professor and Director of the Center for Advanced Technology and Education (CATE), Department of Electrical and Computer Engineering, Florida International University, Miami, FL 33174 USA.

morphological features of the brain. Normalization for varying head sizes reduces the bias on the study results [10]. ICV, along with age and gender, are reported as covariates to adjust for regression analysis in investigating a lot of progressive neurodegenerative brain disorders, such as Alzheimer's disease [10] aging and cognitive impairment [11]. ICV has also been utilized as an independent voxel based morphometric feature to determine characterizing atrophy patterns in subjects with mild cognitive impairment (MCI) and Alzheimer's disease (AD) [12]. ICV is also viewed as a critical normalization factor while analyzing neurological diseases such as Alzheimer [10].

AFNI [13], Freesurfer [14], FSL [15] and SPM [16] are widely accepted and well-known software packages in neuroimaging studies. These different software packages come with specific subroutines for estimating ICV. In assessing the reliability and accuracy of each of these software packages, a first challenge is in determining if the outcome is consistent over the variability exhibited with respect to age, strength of the scanner used, slice sampling considered, controls and patients in the study, and the type of neurological disorder is under study. The main focus of this study is in analyzing the accuracy of publicly available software packages (AFNI version 2011-12-21-1014, FS version 5.1.0, FSL version 5.0 and SPM version 8) for ICV estimation in adults (controls and patients with AD) and children (controls and patients with epilepsy).

## II. MATERIALS AND METHODS

### A. Subjects and Images

Different groups of control subjects and patients diagnosed with a neurological disorder from pediatric and adult populations were considered. The study was approved by the local institutional review board (IRB) and informed consent forms were provided from the subjects or their legal representatives. Table 1 provides a summary of the dataset with the different groups considered in this study: *Pediatric Epilepsy with 1.5T MRIs*, *Pediatric Epilepsy with 3T MRIs* [17], *Pediatric Control*, *Adult with Dementia*, and *Adult Control*.

### B. Reference ICV Estimation ( $ICV_{ref}$ )

Reference ICV ( $ICV_{ref}$ ) measurements were acquired manually by from T1-weighted image volumes, which were performed using an AFNI plugin, by allowing the user to draw volumetric masks. T1-weighted image volumes from each subject were loaded into AFNI as an underlay image. An overlay mask was drawn following every slice protocol to highlight the voxels that belong to ICV [18]. The mask mimicked the segmented boundary of the dura matter. The  $ICV_{ref}$  measure is then calculated by counting the total

TABLE I. A SUMMARY OF THE DATASET USED FOR THE STUDY

	Number of subjects		Age		Diagnosis	Field Strength (T)	Slice Thickness (mm)
	Male	Female	Male	Female			
PE1.5	8	9	8.7±7.1	10.6±6.6	Epilepsy	1.5	1.6
PE3	5	8	11.2±2.5	13.6±2.9	Epilepsy	3	4.0
PC	10	8	10.6±0.7	11.4±1.7	Control	3	1.0
AD	5	6	83.6±7.2	78.2±10.7	Dementia	1.5	1.0
AC	2	9	70.5±3.5	70.7±7.0	Control	1.5	1.0

number of voxels within the mask multiplied by the volume of a single voxel. Figure 1 shows one sagittal slice of T1 weighted image volume and the reference measurement highlighting the ICV segmentation for the same slice for a random subject from the dataset. The arrows in Figure 1 are drawn pointing to the dura border defining the ICV.

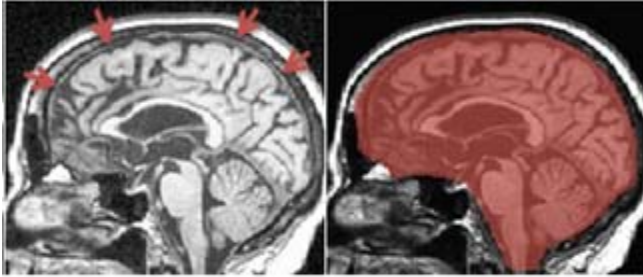


Figure 1. Reference ICV segmentation for one sagittal slice of a random subject, showing the T1 weighted image (left) and the result of manual ICV segmentation. Arrows in the left image point to the dura matter which is being used as boundary marker for segmenting the ICV.

### C. Automatic ICV Estimation Methods

T1-weighted image volumes were used as input to all the automated approaches for estimating ICV. No other external intervention was involved and a set of default parameters (defined by the software) without any tuning were chosen only when required by the software package under consideration. The  $ICV_{AFNI}$  (AFNI version AFNI\_2011\_12\_21\_1014) [13] has a fully automated approach (3dSkullStrip, December 2012 released version) to segment the brain from surrounding tissue, which serves as an estimation of the intracranial region segmentation. The approach implemented here is an updated version of Brain Extraction Tool (BET) algorithm that corrects for non-uniformity artifacts and expands a spherical surface iteratively until all the brain tissue is encircled, but excluding the eyes. Brain extracted images were overlaid on top of the subject's T1-weighted images and the total number of overlap voxels were counted using another AFNI program, 3dmaskave. Automated ICV estimation from AFNI ( $ICV_{AFNI}$ ) was calculated by multiplying the single voxel volume by the number of voxels found from 3dmaskave. All steps were merged into a single script to maintain the fully-automated nature of ICV estimation without external intervention.

The  $ICV_{FS}$  (Freesurfer version 5.1.0): Freesurfer estimate of ICV is atlas-based estimation considering the fact that determinant of the registration matrix used to register subject image to atlas space includes information about corresponding volume changes by applying the registration. Freesurfer default atlas is made of 40 adult subjects including 10 subjects diagnosed with Alzheimer's disease (AD) [18]. Since the ICV of the atlas was given, the FreeSurfer estimate of subject's ICV,  $ICV_{FS}$ , was calculated by dividing the ICV

of the atlas by the determinant of the affine registration matrix driven through the "recon-all" pipeline implemented by FreeSurfer routine [18, 19]. "recon-all" is a fully automated image processing pipeline in FreeSurfer which performs cortical reconstruction process.

The  $ICV_{FSL}$  (FSL version 5.0): The ENIGMA protocol for brain and intracranial volumes<sup>1</sup> as implemented here to estimate ICV using FSL,  $ICV_{FSL}$ , involves an MNI atlas-based estimation procedure. T1 weighted image volume of each subject brain was linearly aligned to MNI152 space. The  $ICV_{FSL}$  measure was then calculated by dividing ICV of the MNI152 brain by the determinant of the affine registration matrix. FSL estimation of ICV involves stripping the images from the skull using BET [20]. The protocol employs a two steps BET with an intermediate FAST (FMRIB's Automated Segmentation Tool<sup>2</sup>) to correct for bias. The fractional intensity threshold was set to default value of 0.5 and threshold gradient was set to default value of 0.  $ICV_{SPM}$  (SPM version 8): VBM toolbox<sup>3</sup> of SPM uses template probability map and segments tissues into four clusters, gray matter, white matter, CSF and other, in native space [16, 18, 19]. SPM estimate of ICV were obtained by summing the volume of first three clusters together.

### D. Statistical Analysis

The means of  $ICV_{AFNI}$ ,  $ICV_{FS}$ ,  $ICV_{FSL}$  and  $ICV_{SPM}$  were tested against the mean of  $ICV_{ref}$  for each of PE1.5, PE3, PC, AD and AC groups through post hoc *t*-tests under the general linear model, using R package *PHIA* [21]. All *p*-values less than the significance level of 0.01 (Bonferroni adjusted) were considered to show the existence of a significant difference. Mean related percentage of absolute difference (MRPAD) in ICV estimation within each group were calculated using equation (1).

$$MRPAD = \frac{1}{n} \sum_{i=1}^n \frac{|\Delta_{aut_i}|}{ICV_{ref_i}} \times 100 \quad (1)$$

where  $\Delta_{aut_i}$  is the error of the automated software in ICV measurement from the reference measurement; *aut* represents the automatic software employed: AFNI, FS, FSL and SPM; *n* is the number of subjects within the group. The  $R^2$  statistics were computed through multiple linear regression analysis. Comparative reliability assessment of automated tools based on *MRPAD* alone could be biased due to the fact that *MRPAD* is not sensitive to the segmentation accuracy. To account for the segmentation error in a more effective way, metrics of Dice Coefficient (DICE), %Under (percent of underestimation) and %Over (percent of overestimation) caused by the automatic software were

<sup>1</sup> www.enigma.ini.usc.edu.

<sup>2</sup> www.fsl.fmrib.ox.ac.uk/fsl.

<sup>3</sup> www.fil.ion.ucl.ac.uk/~john/misc/VBMclass10.pdf

considered to overcome the issue of reliability assessment only based on absolute error.

### III. RESULTS AND DISCUSSION

Paired t-test statistics comparing within-subjects ICV estimated from each automated tool and reference for each group along with MRPAE values are given in Table II. Table III provides the segmentation accuracy assessment of each automated tool. For comparison purposes, tools are grouped into Atlas based and Non-Atlas based estimation considering the protocol they follow for estimating ICV. The p-value less than the significance level of 0.01 (Bonferroni adjusted) were highlighted to show the existence of statistically significant differences. The sign of t statistics indicates how the automated measurements are biased comparing with respect to the reference, and the p value shows if the bias is significant or not. In the current study, a negative t statistics indicates an upward bias and vice versa, whereas a p-value higher than threshold (0.01) is deemed as a good measure as there is no statistically significant mean difference between the two compared groups. In light of this, it can be seen from Table II that all automated measurements had no statistically significant difference in means as compared with the reference for PE 1.5 groups, whereas the opposite is seen for PE 3 group where all automated measurements turned out to be significantly different from reference ICV measurement.

For PE1.5 group, statistical testing does not show significant difference for software packages except for FSL which could be due to the small sample size; however, variability in reference ICV is best explained by FSL ( $R^2 = 0.61$ ) which has the lowest MRPAD value among the software types used. FS and SPM failed in estimating ICV for part of the PE1.5, which we believe were partly due to the low resolution of the MRI images.

For PE3 group, empirical observation supports that all tools (AFNI:  $p < 0.01$ , FS:  $p < 0.01$ , FSL:  $p < 0.01$ , and SPM:  $p < 0.01$ ;) underestimated the reference ICV. FSL ( $R^2 = 0.6$ ) and AFNI ( $R^2 = 0.57$ ) are more able to explain the variance of reference ICV within the group.

The situation remains the same for PC group where all tools (AFNI:  $p < 0.01$ , FS:  $p < 0.01$ , FSL:  $p < 0.01$ , and SPM:  $p < 0.01$ ;) significantly biased the reference ICV downward, with AFNI ( $R^2 = 0.97$ ) and FSL ( $R^2 = 0.95$ ) providing a better fit in modeling reference ICV. In general, FSL showed to be a better candidate for pediatric populations. The introduced bias may be due to the scaling

factor which FSL employs to translate the estimated ICV in the atlas space into the native space.

For AD group, FSL ( $p < 0.01$ ) overestimates the ICV whereas SPM ( $p < 0.01$ ) underestimates it. FS ( $R^2 = 0.46$ ) and FSL ( $R^2 = 0.46$ ) resulted in a similar  $R^2$  value in predicting reference ICV, however FS biases less the reference ICV than FSL. FS showed to work best among other automated tools in explaining the variance found in the reference ICV. Coefficient of determination for the fit generated by FSL was similar to the one for FS, with FS deemed a better tool due to the bias generated by FSL.

For AC group, ICV measurements calculated using FSL ( $p = 0.01$ ) upwardly biases the reference ICV estimates, but AFNI ( $p < 0.01$ ) and SPM ( $p < 0.01$ ) underestimate the reference ICV. FS ( $R^2 = 0.67$ ) explains the variance of the reference ICV better than the other automated tools for AC group and has the lowest MRPAD value.

### IV. CONCLUSION

Four publicly available software packages were contrasted against a manual reference to measure their reliability in automatically estimating ICV across different groups of subjects. The study emphasizes the importance in the choice of the right sampling period in the manual estimation of ICV and the selection of the right software tool in the automated estimation of ICV, which are shown to depend largely on the demographics of the targeted population, the imaging parameters of the MR machine, as well as the neurological disorder under study. The other important finding of the study was the proper setting of the parameters involved in the process of ICV estimation when they are required. Self-tuning of the parameters for each dataset is highly suggested based on the finding of the study to reduce the bias in the automated ICV estimation. The current study serves as an initial framework for establishing and appropriate protocol in automatic ICV estimation under different imaging conditions and with different populations.

Dataset with more number of subjects (specifically in PE1.5 group) would enhance the reliability of the statistics for future consideration. As ICV has gained its popularity and showed its significance in research area of Alzheimer [22, 23] and epilepsy [24-26], the study could serve as an important guide for the researchers to choose the most effective measurement approach for the automated estimation of ICV.

TABLE II. PAIRED T-TEST STATISTICS COMPARING WITHIN-SUBJECTS ICV ESTIMATED FROM EACH AUTOMATED TOOL AND REFERENCE FOR EACH GROUP ALONG WITH MRPAD VALUES

	PE1.5		PE3		PC		AD		AC	
	Statistics	MRPAD	Statistics	MRPAD	Statistics	MRPAD	Statistics	MRPAD	Statistics	MRPAD
Non-Atlas Based										
"Ref" vs "AFNI"	t = 0.6 p = 0.58	14.37	t = <b>5.97</b> p < 0.01	12.77	t = <b>15.47</b> p < 0.01	9.48	t = 1.4 p = 0.19	13.29	t = <b>3.2</b> p < 0.01	13.15
"Ref" vs "FSL"	t = <b>4.75</b> p < <b>0.01</b>	12.57	t = <b>6.29</b> p < 0.01	13.41	t = <b>13.37</b> p < 0.01	11.35	t = <b>-10.19</b> p < 0.01	91.8	t = -3.16 p = 0.01	41.74
Atlas Based										
"Ref" vs "SPM"	t = 3.8 p = 0.018	21.33	t = <b>5.74</b> p < 0.01	16.64	t = <b>6.67</b> p < 0.01	20.37	t = <b>3.18</b> p < 0.01	12.55	t = <b>6.01</b> p < 0.01	10.15
"Ref" vs "FS"	t = 2.81 p = 0.048	32.17	t = <b>15.23</b> p < 0.01	43.9	t = <b>22.91</b> p < 0.01	30.35	t = 1.8 p = 0.1	9.69	t = 1.63 p = 0.13	5.49

TABLE III. SEGMENTATION ACCURACY ASSESSMENT (DICE, %UNDER AND %OVER) OF EACH AUTOMATIC TOOL (AFNI, FSL, FS AND SPM)

Non-Atlas Based	AFNI			FSL		
	DICE	%Under	%Over	DICE	%Under	%Over
PE1.5	0.92	9.05	7.26	0.94	5.05	5.99
PE3	0.95	3.38	7.08	0.95	4.49	5.93
PC	0.96	3.6	3.7	0.95	4.47	5.41
AD	0.92	8.18	6.7	0.87	16.21	8.84
AC	0.94	5.78	5.48	0.89	13.12	9.03
Atlas Based	FS			SPM		
	DICE	%Under	%Over	DICE	%Under	%Over
PE1.5	0.94	6.13	6.15	0.95	5.73	2.5
PE3	0.93	3.47	10.41	0.94	4.44	6.94
PC	0.97	3.32	3.7	0.94	6.78	4.3
AD	0.93	7.56	5.51	0.96	4.45	2.93
AC	0.94	7.83	4.47	0.96	4.65	2.49

ACKNOWLEDGMENT

This work is supported by the National Science Foundation under grants CNS-0959985, CNS-1042341, HRD-0833093, and IIP-1230661. The support of the Ware Foundation is greatly appreciated.

REFERENCES

[1] J. Eritaia, S.J. Wood, N. Bridle, P. Dudgeon, P. Maruff, D. Velakoulis, C. Pantelis, "An optimized method for estimating intracranial volume from magnetic resonance images," in *Magn. Reson. in Med*, 2000, 44(6), pp. 973-977.

[2] R. L. Buckner, D. Head, J. Parker, A.F. Fotenos, D. Marcus, J.C. Morris, A.Z. Snyder, "A unified approach for morphometric and functional data analysis in young, old, and demented adults using automated atlas-based head size normalization: reliability and validation against manual measurement of total intracranial volume," in *NeuroImage*, 2004, 23 (2), pp. 724-738.

[3] N.A. Kochan, M. Breakspear, M. Valenzuela, M.J. Slavin, H. Brodaty, W. Wen, J.N. Trollor, A. Turner, J.D. Crawford, P.S. Sachdev, "Cortical responses to a graded working memory challenge predict functional decline in mild cognitive impairment," in *Biol. Psychiatr.* 2011, 70 (2), pp. 123-130.

[4] A.R. Groves, S.M. Smith, A.M. Fjell, C.K. Tamnes, K.B. Walhovd, G. Douaud, M.W. Woolrich, L.T. Westlye, "Benefits of multi-modal fusion analysis on a large-scale dataset: life-span patterns of inter-subject variability in cortical morphometry and white matter microstructure," in *NeuroImage*, 2012, 63, pp. 365-380.

[5] V. Garibotto, B. Borroni, C. Agosti, E. Premi, A. Alberici, S.B. Eickhoff, S.M. Brambati, G. Bellelli, R. Gasparotti, D. Perani, "Subcortical and deep cortical atrophy in frontotemporal lobar degeneration," in *Neurobiol. of aging*, 2011, 32 (5), pp. 875-884.

[6] A.M. Graca, K.R.V. Cardoso, J.M.F.P da Costa, F. M. Cowan, "Cerebral volume at term age: Comparison between preterm and term-born infants using cranial ultrasound," in *Early Hum. Dev.*, 2013, 89, pp. 643-648.

[7] A.G. Ritvanen, M.E. de Oliveira, M.P. Koivikko, H.O. Hallila, J.K. Haaja, V.S. Koljonen, J.P. Leikola, J.J. Hukki, M.M. Paulasto-kröckel, "Mesh-based method for measuring intracranial volume in patients with craniostylosis," *Int. j. of Comput. Assist. Radiol. Surg.*, 2013, pp. 1-7.

[8] O.F. Sonmez, Y. Temel, V. Visser-Vandewalle, B. Sahin, E. Odacı, "A new evaluation method for the intracranial volume changes and subdural effusion of patients following endoscopic third ventriculostomy," *Clinic. Neurol. and Neurosurg.*, 2013, 115 (2), pp. 160-164.

[9] M.A. Ikram, M. Fornage, A.V. Smith, S. Seshadri, R. Schmidt, S. Debette, H.A. Vrooman, S. Sigurdsson, S. Ropele, H.R. Taal, "Common variants at 6q22 and 17q21 are associated with intracranial volume," *Nat. Genet.*, 2012, 44 (5), 539-544.

[10] E. Westman, C. Aguilar, J-S. Muehlboeck, A. Simmons, "Regional magnetic resonance imaging measures for multivariate analysis in Alzheimer's disease and mild cognitive impairment," *Brain Topogr.*, 2013, 26 (1), pp. 9-23.

[11] M.A. Trivedi, T.R. Stoub, C.M. Murphy, S. George, R.C. Shah, S. Whitfield-Gabrieli, J.D. Gabrieli, G.T. Stebbins, "Entorhinal cortex

volume is associated with episodic memory related brain activation in normal aging and amnesic mild cognitive impairment," *Brain Imaging and Behav.* 2011, 5 (2), pp. 126-136.

[12] M. Thambisetty, Y. An, A. Kinsey, D. Koka, M. Saleem, A. Güntert, M. Kraut, L. Ferrucci, C. Davatzikos, S. Lovestone, "Plasma clusterin concentration is associated with longitudinal brain atrophy in mild cognitive impairment," *NeuroImage*, 2012, 59 (1), pp. 212-217.

[13] R.W. Cox, "AFNI: software for analysis and visualization of functional magnetic resonance neuroimages," *Comput. and Biomed. Res.*, 1996, 29 (3), pp. 162-173

[14] A.M. Dale, B. Fischl, M.I. Sereno, "Cortical surface-based analysis: I. Segmentation and surface reconstruction," *NeuroImage*, 1999 9 (2), pp. 179-194.

[15] M. Jenkinson, C.F. Beckmann, T.E.J., Behrens, M.W. Woolrich, S.M. Smith, "FSL," *NeuroImage*, 2012, 62 (2), pp. 782-790.

[16] Ashburner, J., Friston, K.J., "Unified segmentation," *NeuroImage*, 2005, 26 (3), pp. 839-851.

[17] X. You, M. Adjouadi, M.R. Guillen, M. Ayala, A. Barreto, N. Rishe, J. Sullivan, D. Dlugos, J. VanMeter, D. Morris, "Sub-patterns of language network reorganization in pediatric localization related epilepsy: A multisite study," *Hum. Brain. Mapp.*, 2011, 32 (5): pp. 784-799.

[18] G. Pengas, J. Pereira, G.B. Williams, P.J. Nestor, "Comparative reliability of total intracranial volume estimation methods and the influence of atrophy in a longitudinal semantic dementia cohort," *J. of Neuroimaging*, 2009, 19 (1), pp. 37-46.

[19] R. Nordenskjöld, F. Malmberg, E.M. Larsson, A. Simmons, S.J. Brooks, L. Lind, H. Ahlström, L. Johansson, J. Kullberg, "Intracranial volume estimated with commonly used methods could introduce bias in studies including brain volume measurements," *NeuroImage*, 2013, 83, pp. 355-360.

[20] M. Jenkinson, C.F. Beckmann, T.E.J. Behrens, M.W. Woolrich, S.M. Smith, "FSL," *NeuroImage*, 2012, 62 (2), pp. 782-790.

[21] H. De Rosario-Martinez, "PHIA: Post-Hoc Interaction Analysis. R package version 0.1-0," <http://CRAN.R-project.org/package=phia>.

[22] Q. Zhou, M. Goryawala, M. Cabrerizo, J. Wang, W. Barker, D. Loewenstein, R. Duara, M. Adjouadi, "An Optimal Decisional Space for the Classification of Alzheimer's Disease and Mild Cognitive Impairment," *IEEE Trans. on Biomedical Engineering*, 2014, 8 pages, DOI: 10.1109/TBME.2014.2310709.

[23] Q. Zhou, M. Goryawala, M. Cabrerizo, W. Barker, R. Duara and M. Adjouadi, "Significance of Normalization on Anatomical MRI Measures in Predicting Alzheimer's Disease," *The Scientific World Journal*, 2014, 12 pages Article ID 541802.

[24] S. Keihaninejad, A.H. Rolf, F. Gianlorenzo, R.S. Mark, V.H. Joseph and A. Hammers, "A robust method to estimate the intracranial volume across MRI field strengths (1.5 T and 3T)," *Neuroimage*, 2010, 50, no. 4, pp. 1427-1437.

[25] M. Cabrerizo, M. Ayala, M. Goryawala P. Jayakar, and M. Adjouadi, "A New Parametric Feature Descriptor for the Classification of Epileptic and Control EEG Records in Pediatric Population," *International Journal of Neural Systems*, 22:2 (16 pages), DOI: 10.1142/S0129065712500013.

[26] N. Mirkovic, M. Adjouadi, I. Yaylali, and P. Jayakar, "3-D Source Localization of Epileptic Interictal Spikes," 2003, *Brain Topography*, 16 (2): pp. 111-119.